Catalysis Letters 7 (1990) 27–52

HYDROGEN ADSORPTION ON SUPPORTED COBALT, IRON, AND NICKEL

Calvin H. BARTHOLOMEW

BYU Catalysis Laboratory, Department of Chemical Engineering, Brigham Young University, Provo, Utah 84602, U.S.A.

Adsorption, H_2 on supported Co, Fe, and Ni; chemisorption, H_2 on supported Co, Fe, and Ni; adsorption, H_2, reversibility and stoichiometry of on base metals; surface area, of bases metals by H_2 adsorption

This paper emphasizes concepts and fundamentals relating to the kinetics, energetics, and stoichiometries of adsorption of hydrogen on supported cobalt, iron and nickel, with emphasis on nickel. Relationships between catalyst and adsorption properties and the application of hydrogen chemisorption to the measurement of metal surface areas are discussed. Evidence is presented for nonstoichiometric adsorption of hydrogen on supported metals and the results are interpreted in terms (i) reversibility of adsorption and (ii) interactions of hydrogen with metal oxides present on or near metal crystallites. Contamination of the metal surface by support moieties can cause (i) the appearance of new adsorption states of hydrogen at higher binding energies and (ii) an increase in the adsorption activation energy for hydrogen which can lead to severe kinetic limitations in the adsorption process. Precalcination treatments and promoters such as potassium also cause the appearance of new high temperature adsorption states and significantly increase the adsorption activation energy for hydrogen.

1. Introduction

Hydrogen plays a significant role as a reactant or product in many important catalytic processes: moreover it is used widely as a selective chemisorbate to measure surface areas of catalytic metals. A recently published book "Hydrogen Effects in Catalysis, Fundamentals and Practical Applications," [1] provides a comprehensive review of many aspects of hydrogen catalysis and adsorption. Chapter 5 of that book is a somewhat more comprehensive treatment of the subject presented in this paper.

In this paper evidence for nonstoichiometric adsorption of hydrogen on supported metals will be discussed and interpreted in terms (i) reversibility of adsorption and (ii) changes in the kinetics and energetics of hydrogen adsorption due to the presence on the metal surface of support moieties or metal oxides.

This paper also addresses several other important issues:

1. The influence of (i) the interaction between metal and support, (ii) promoters, and (iii) preparation on the kinetics, energetics, and stoichiometry of hydrogen adsorption.
2. Dependence of reversible hydrogen adsorption on the temperature of adsorption, crystallite size, and metal loading.
3. The best methods and their limitations for measuring monolayer hydrogen adsorption on supported base metals.
4. Complications introduced by unreduced metal oxide phases in estimating dispersion of base metal/support systems and possible treatments of these complications.

2. Kinetics and energetics of adsorption

A. CALORIMETRIC AND TPD STUDIES OF HYDROGEN INTERACTION WITH SUPPORTED Ni

Early calorimetric studies of hydrogen adsorption on nickel involved metallic films [2–7]. While numerous TPD studies of hydrogen from single crystal nickel have been reported [2,8–12], relatively few TPD studies of hydrogen from supported nickel have been published [13–18]. Four of these studies involving high surface area catalysts [15,16] or nickel films [17,18] were conducted in the clear absence of transport influences [19–23] and in the case of high surface area samples, took into account readsorption of hydrogen on the metal crystallites [15,16,20–22], thus providing quantitative kinetic data. The results of these studies are summarized and compared with data from single crystal TPD and calorimetric film studies in table 1. Fig. 1 shows thermal desorption spectra for hydrogen on Ni (100) according to Christmann [11] while figs. 2–5 show TPD spectra of nickel supported on titania and alumina.

To facilitate the discussion of these results and to provide a foundation for discussion of material in sections to follow, a brief review of the fundamentals of hydrogen adsorption on single crystal nickel is useful. Two atomic states are observed for hydrogen adsorption on Ni (100), Ni (110), and Ni (111) which desorb in the range of 180–450 K [10,12]. The β_2 state forms at low coverages, while the β_1 state forms after β_2 at higher coverages (see fig. 1). Fig. 1 shows that the maximum rate of desorption for the β_1 state occurs near room temperature; accordingly the β_1 state is easily desorbed at room temperature [10] and will therefore not be observed in TPD studies in which hydrogen was adsorbed at room temperature followed by purging in inert gas (e.g. the studies in refs. [15,16]). According to Christman et al. [11] hydrogen adsorption is completely reversible at room temperature. Saturation coverage of hydrogen at 120–180 K (β_1 and β_2 states) corresponds to 0.9–1.0 monolayers [11,12], i.e. a H/Ni_s ratio

Table 1
Atomic TPD states and heats of adsorption of hydrogen on nickel surfaces

Surface	Temperature maxima (K) of atomic states observed by TPD			Desorption order	$-\Delta H_a$ [a] (kJ/mole)	Ref.
	β_1	β_2	γ			
Ni (100)	300–325	350–400	–	2	96 [b] (β_2)	[10,11]
Ni (110)	–	350–360	–	1	90 [b] (β_2)	[10]
Ni (111)	320–340	360–395	–	2	96 [b] (β_2)	[10]
Polycrystalline Ni	–	–	–		75–130 [c]	[2]
Ni	–	410 ($\theta = 0.5$)	–		87 [d]	[16]
24% Ni/SiO_2	334 ($\theta = 1$)	450 ($\theta = 1$)	620 ($\theta = 1$)		61 [d], 85 [d], 123 [d]	[14]
50% Ni/SiO_2	–	450–575	–	2	89 [e]	[15]
50% Ni/SiO_2	–	425 ($\theta = 0.5$)	–	2	87 [e]	[16]
10% Ni/SiO_2	–	415 ($\theta = 0.5$)	–	2	82 [e]	[16]
3% Ni/SiO_2	–	410 ($\theta = 0.5$)	–	–	82 [d]	[16]
14% Ni/Al_2O_3	–	335 ($\theta = 0.5$)	605 ($\theta = 0.5$)	–	70 [d], 125 [d]	[16]
0.7 ML [f] Al_2O_3/Ni	275	350–375	450	–	–	[17]
10% Ni/TiO_2	–	375 ($\theta = 0.5$)	520 ($\theta = 0.5$)	–	84 [d], 105 [d]	[16]
1 nm Ni/TiO_2	–	425 [g]	500 [g]	–	–	[18]
0.3 ML [f] TiO_2/Ni	–	360	480	2	75, 108	[17]

[a] Heat of adsorption or activation energy.
[b] Activation energies from flash desorption.
[c] Heats of adsorption by calorimetry.
[d] Heats of adsorption estimated from desorption peak temperatures according to method of Konvalinka (ref. [14]) which accounts for readsorption.
[e] Heats of adsorption using desorption rate isotherms extrapolated to low coverage and assuming readsorption in quasi-equilibrium.
[f] ML = units of monolayer coverage.
[g] Reduced in hydrogen at 820 K.

of essentially unity. Finally, it is clear that there are only small differences in the binding energies for hydrogen on the three lowest index planes of nickel (see table 1); in other words the energetics of adsorption are little affected by surface structure, at least on the three lowest index planes.

The data in table 1 reveal some important similarities and differences for the kinetics and energetics of hydrogen adsorption on supported nickel relative to single crystal nickel. Based on the recent quantitative TPD studies [15,16] hydrogen adsorption on Ni/silica at room temperature involving half monolayer coverage is very similar to that on single crystal surfaces, as evidenced by the appearance of a single β_2 peak having a desorption order of 2 and a heat of adsorption (82–89 kJ/mole) very nearly the same as for the single crystal surfaces (90–96 kJ/mole). The shift to higher temperatures for the peak maximum for the β_2 state on Ni/silica relative to single crystal nickel is most probably a result of readsorption on the supported catalysts [20–22].

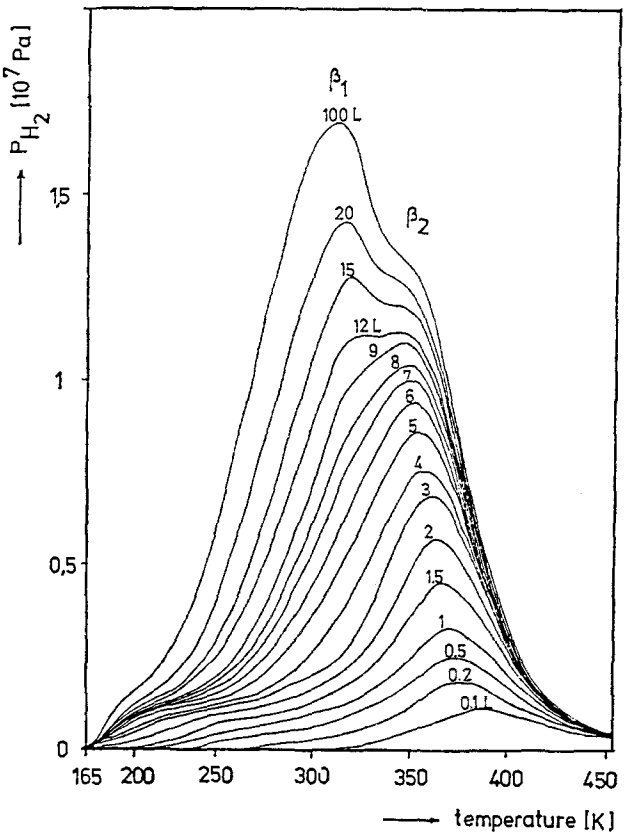

Fig. 1. Thermal desorption spectra for the β_1 and β_2 states of hydrogen on a nickel (100) surface. Parameter is the exposure (L) ([ref. [11]).

The TPD spectrum for 130 K adsorption to greater than a monolayer of hydrogen on a 24% Ni/silica (ref. [14]) consists of mainly 2 low temperature peaks (weakly absorbed α states) and 3 large peaks above room temperature corresponding to moderately or strongly adsorbed hydrogen. The peak at 334 K with an adsorption heat of 61 kJ/mole can be assigned to the β_1 state and that at 450 K (heat of adsorption of 85 kJ/mole) to the β_2 state. However, the observation of the γ state reported at 620 K (heat of adsorption of 123 kJ/mole) for Ni/silica is unique to this study; this could be a result of the preparation procedure involving precipitation and calcination–the latter treatment possibly causing a shift in adsorption states to higher temperatures [24]. The assignment of this high temperature state by Konvalinka et al. [14] to edge and corner sites on small crystallites in their sample is unlikely in view of the structure insensitivity of hydrogen adsorption discussed above but cannot be ruled out altogether.

The adsorption of hydrogen on Ni/titania and Ni/alumina is clearly more complicated than that on single crystal nickel or nickel/silica (see table 1 and figs. 2–5). In both of these systems, two strongly bound states β_2 and γ, are

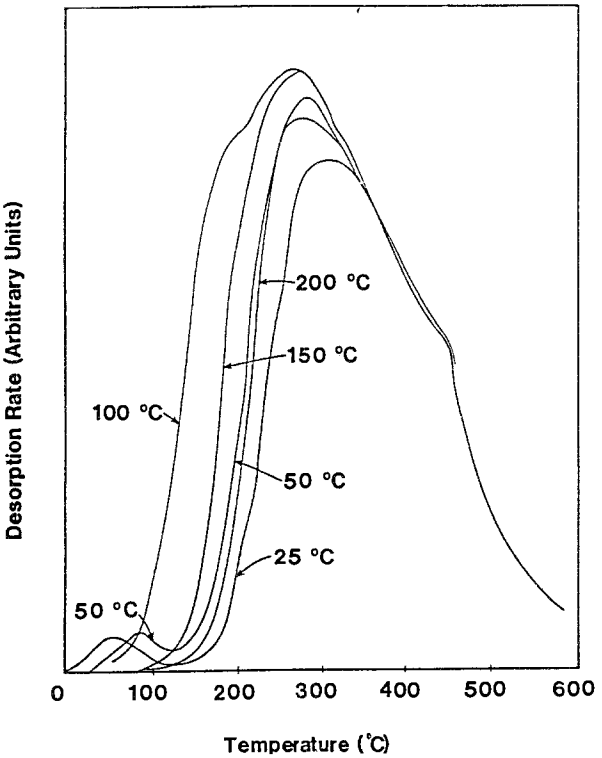

Fig. 2. Hydrogen TPD spectra for 14% Ni/alumina at different adsorption temperatures ([ref. [16]).

observed after hydrogen adsorption at 300 K (figs. 2 and 4); the high temperature γ state is the predominant peak in both of these catalysts reduced at 673 and 725 K respectively. Moreover, the appearance of a distinct shoulder at about 700 K (450 °C) in the spectra for hydrogen desorption from 14% Ni/alumina (fig. 4) provides evidence for the existence of γ_1 and γ_2 states at approximately 600 and 700 K respectively. One or both of these states apparently involves activated adsorption, since the TPD spectral area increases with increasing adsorption temperature. Raupp and Dumesic [17] observed similarly that alumina on nickel (70% of a monolayer, prepared by sputtering aluminum on the surface of a nickel film, followed by oxidation and reduction) causes the appearance of a new γ state at 400–500 K after hydrogen adsorption at 300 K but not after adsorption at 150 K (see fig. 3). In other words, there is an activation barrier for adsorption into the strongest adsorption state. Thus, adsorption of hydrogen on the alumina-coated nickel film is very similar to that of the 14% Ni/alumina.

Adsorption of hydrogen on nickel is generally assumed to be nonactivated, i.e., to have near zero activation energy and thus no kinetic barrier to adsorption [25]. Indeed, Roberts [26] observed an activation energy for adsorption of hydrogen on nickel wire of only 1.7 kJ/mole. Moreover, the kinetics of adsorption/desorption from hydrogen on single crystal nickel [7–12] and Ni/silica [15,16] are consistent

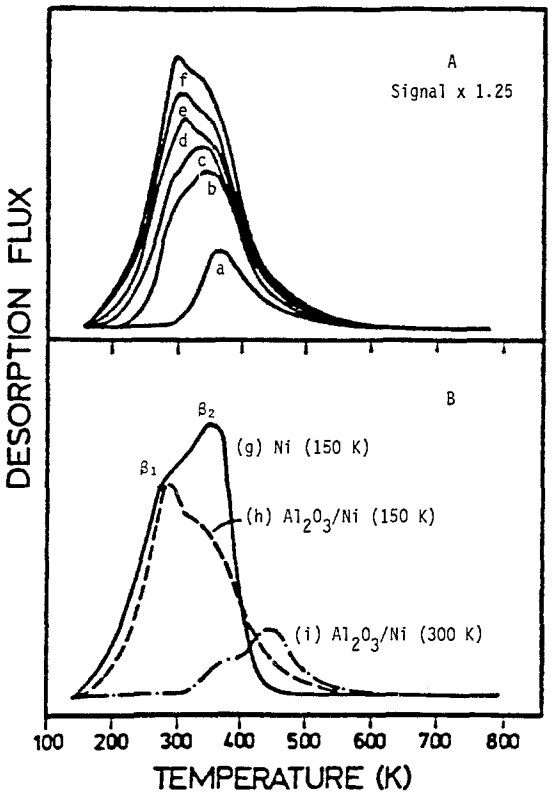

Fig. 3. (A). Hydrogen desorption from alumina/Ni following different hydrogen exposures at 150 K: (a) 0.3, (b) 1.0, (c) 3.0, (d) 5.0, (e) 13, and (f) 30 L. Alumina coverage was 0.7 ML. (B). Hydrogen desorption from saturàtion coverage on (g) clean Ni dosed at 150 K, (h) alumina/Ni dosed at 150 K, and (i) alumina/Ni dosed at 300 K ([ref. [17]).

with this assumption; indeed the amount adsorbed decreases with increasing temperature above about 120 K for these systems, since adsorption and desorption are in a near equilibrium which under these conditions favors desorption. However, in the case of 14% Ni/alumina (fig. 2) the activation energy for hydrogen adsorption is significant, i.e. 10 kJ/mole [16]. The higher activation barrier to hydrogen adsorption on Ni/alumina and the appearance of new adsorption states at higher binding energies is probably best explained by the presence of unreduced nickel and aluminum oxide species on the nickel surface or in intimate contact with small nickel crystallites [17,18,24,27,28]. This hypothesis is strongly supported by the similarity in TPD spectra for Ni/Al_2O_3 and Al_2O_3/Ni discussed above. It is well known that nickel supported on alumina is more difficult to reduce to the metallic state than nickel on silica [29,30]. The greater apparent adsorption strength of these sites may be partially due to steric hindrance by these contaminant species of hydrogen atoms during surface diffusion and recombination [17] while the increase in activation energy for adsorption

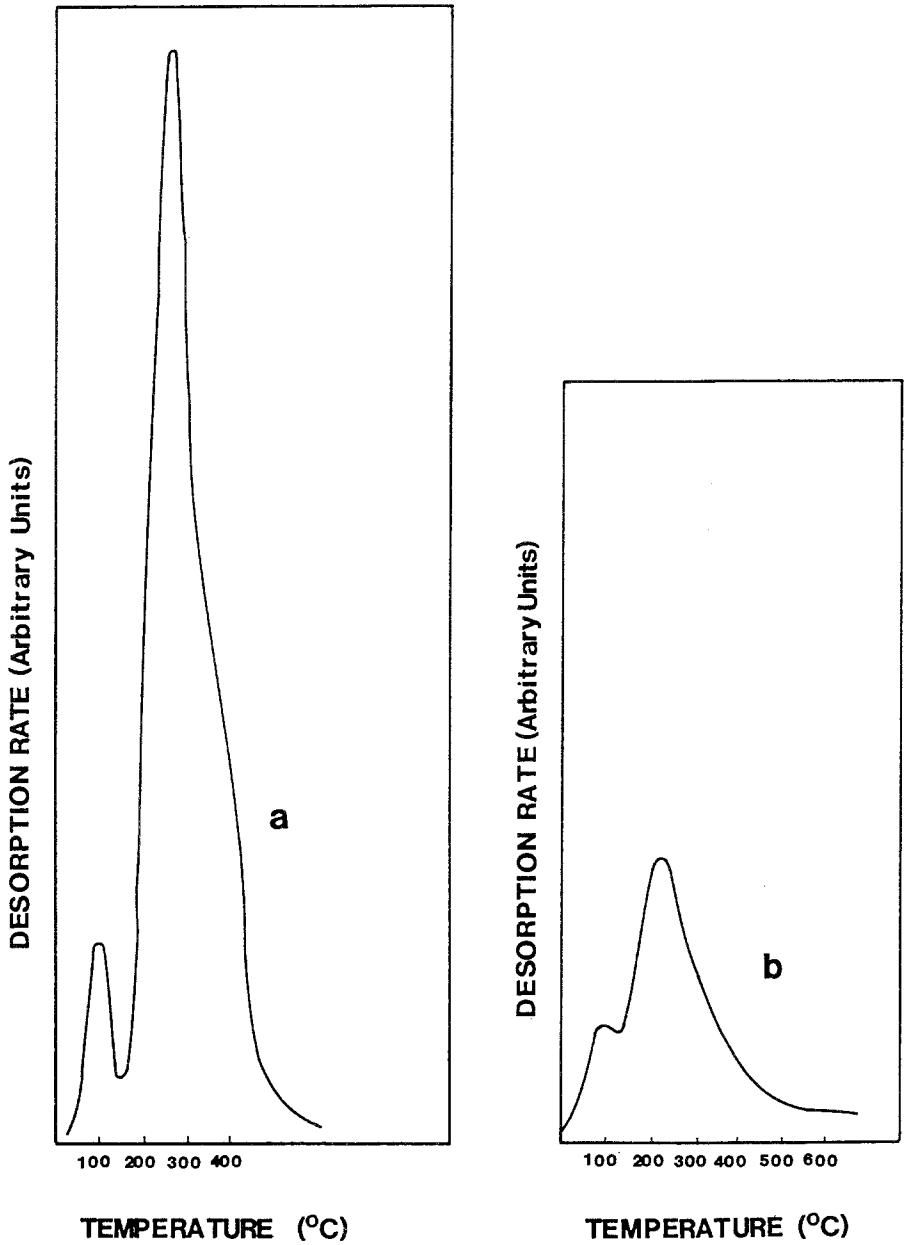

Fig. 4. Hydrogen TPD spectra for 10% Ni/titania: (a) After reduction at 400°C; (b) After successive reductions of 1 h each at 400, 500, 600 and 700°C; desorption rates are on the same scale for both runs ([ref. [16]).

occurs as a result of local interactions of nickel sites with neighboring nickel or aluminum oxide species [17]. The presence of other adlayer species such as carbon, copper and potassium has been shown to induce activation energy

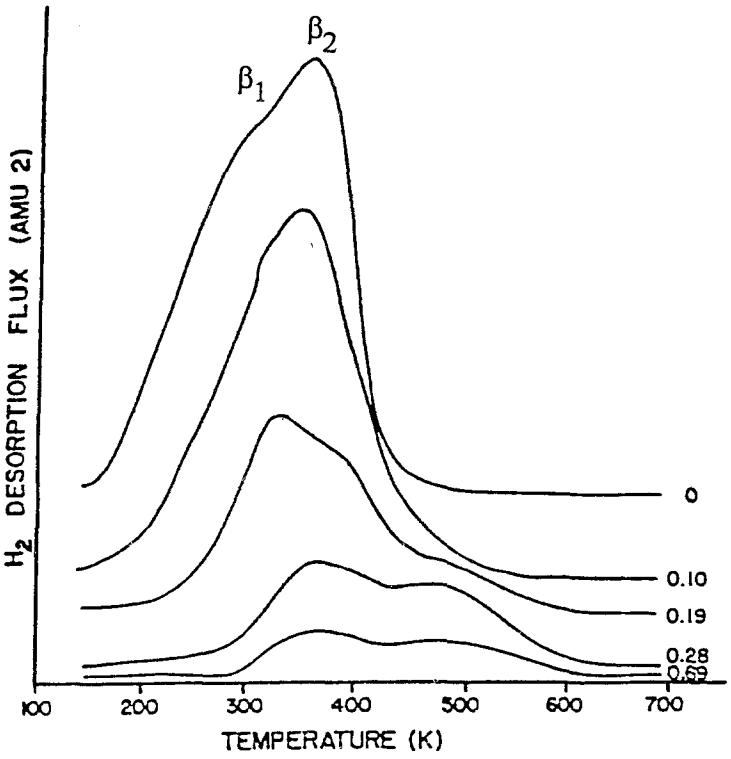

Fig. 5. Effect of varying TiO_x coverage on hydrogen thermal desorption from nickel following saturation hydrogen exposure at 150 K ([ref. [17]).

barriers for hydrogen adsorption on Ni and in the case of potassium to increase binding energies, although carbon and copper species decrease binding energies [17,24,31].

The behavior of Ni/titania for hydrogen adsorption is similar to that of Ni/alumina, although the observed effects of support are more dramatic and more sensitive to reduction temperature in the former system. In the case of a 10% Ni/titania catalyst reduced initially at 673 K, there is a dramatic decrease in the intensity and area of the beta and gamma peaks with increasing reduction temperature (see fig. 4). Raupp and Dumesic [18] found that hydrogen adsorption on a 1 nm nickel film overlaying a titania film was very similar to that on single crystal nickel; however, as the nickel film/titania film was heated to progressively higher temperatures in hydrogen, the saturation coverage decreased while the peak maximum shifted to higher binding energies (see table 1).

The decrease in saturation hydrogen coverage and shift to higher binding energies for the Ni/titania system can be attributed to decoration of the nickel surface with reduced TiO_x species [17,18]. Indeed, Raupp and Dumesic [17] found that titania on a nickel film behaved similarly to Ni/titania; as the titania coverage was increased progressively to about two-thirds of a monolayer, the

hydrogen TPD spectrum transformed from one typical of single crystal nickel with β_1 and β_2 peaks at 300 and 400 K respectively to one involving two states of higher binding energy but of lower occupancy (see fig. 5). Moreover, upon adsorption of hydrogen at 300 K on the samples of higher TiO_x coverage, a new activated state was observed at higher binding energies which was attributed to adsorption on sites adjacent to the TiO_x species or to spillover onto the titania support [17]. The observed increased binding energy for the new states observed on nickel decorated with titania might be a consequence of direct bonding of hydrogen adatoms to oxygens associated with surface titania species [17], of a steric hindrance to hydrogen adatom migration and recombination [17], or localized electronic effects in the vicinity of TiO_x species.

Together the results for Ni/alumina and Ni/titania systems reveal a pattern that might well explain two important problems in catalysis: (i) metal support interactions in conventional high-surface area catalysts [17] and (ii) "hydrogen effects" [1] which are sometimes manifest by strongly bound states of hydrogen on these catalysts after reduction at high temperatures. As pointed out by Raupp and Dumesic [17], the underlying cause of "metal-support interactions" or "strong metal-support interactions" involving either so-called "reducible" or "unreducible" supports may be the "contamination or decoration" of the surfaces of metal crystallites by "moieties of the support material." These decorating species, in turn, introduce new hydrogen adsorption states having significantly higher binding energies and activation energies for adsorption. These "high temperature states" can significantly alter the behavior of these supported catalyst systems in chemisorption titrations involving hydrogen and in many important catalytic reactions involving hydrogen as a reactant.

B. CALORIMETRIC AND TPD STUDIES OF HYDROGEN INTERACTION WITH SUPPORTED Co AND Fe

As in the case of nickel, previous calorimetric studies of hydrogen adsorption on cobalt and iron were limited to unsupported powders, filaments, or films [2]. Published TPD studies of hydrogen interaction with supported Co [32–34] and Fe [24,35,36] include only 6 studies from 3 laboratories. Quantitative kinetic and heats of adsorption data, obtained in two of the studies of cobalt [32,34] are summarized and compared with calorimetric [37] and film/single crystal TPD [38,39] data in table 2.

The desorption spectrum for 10% Co/silica after hydrogen adsorption at 298 K (fig. 6) consists of two states, β_2 and β_3, having desorption maxima at 323 and 513 K respectively. At higher adsorption temperatures (e.g., 326 and 373 K) the population of the β_2 state decreases while that of the β_3 increases very significantly indicating that this higher temperature state is activated. Maximum adsorption capacity is observed at about 373 K. This highly activated adsorption state for hydrogen is observed for unsupported cobalt and cobalt supported on

Table 2
Activation energies and heats of adsorption and desorption for H_2/cobalt

Catalyst	E_{Aa} (kJ/mol) [a]	E_{Ad} (kJ/mol) [b]	$-\Delta H_a$ [c]	Order of desorption	Ref.
Unsupported Co	5.8	151	145 ± 10	2	[34]
3% Co/SiO_2	43		–	–	[34]
10% Co/SiO_2	18	168	145 ± 7	2	[34]
10% Co/Al_2O_3	39	144	105	2	[34]
4% Co/TiO_2 (Rutile)		88/138			[32]
Reduced Co (calorimetric)			105		[37]
Co films (surface pot./TPD)		42/79			[38]
Single crystal Co (0001)		67		2	[39]

[a] Activation energy for adsorption of H_2.
[b] Activation energy for desorption of H_2.
[c] Heat of adsorption, $-\Delta H_a = E_{Ad} - E_{Aa}$.

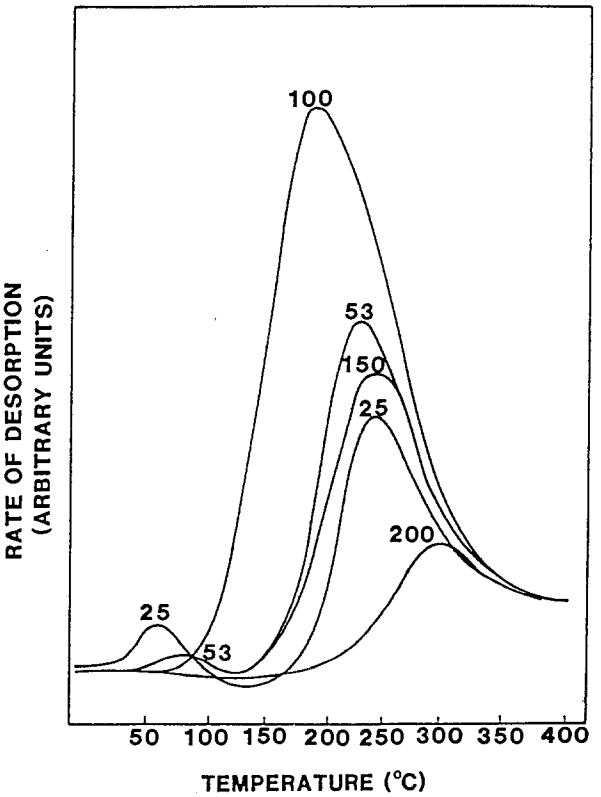

Fig. 6. Hydrogen TPD spectra for 10% Co/silica as a function of adsorption temperature ([ref. [34]).

silica, alumina, titania, and carbon [34]. In Co/MgO and Co/ZSM-5 systems the kinetic limitations are so severe that adsorption is not observed even at elevated temperature except after long periods of exposure to hydrogen [34]. Activation energies for *adsorption* (table 2) range from 5.8 kJ/mole for unsupported cobalt to 39 kJ/mole for 10% Co/alumina and 43 for 3% Co/silica; adsorption activation energies increase with decreasing loading and in the order Co, Co/silica, Co/alumina (if loading is held constant in the supported systems). This order is the same as that for increasing degree of interaction of cobalt with the support.

Activation energies for desorption from the β_3 state, obtained in studies of cobalt, Co/silica, Co/alumina, and Co/titania in which activated adsorption was accounted for [32,34], range from 138 to 168 kJ/mole (table 2). The E_d values (table 2) of 79 and 76 kJ/mole reported for a Co film [38] and single crystal

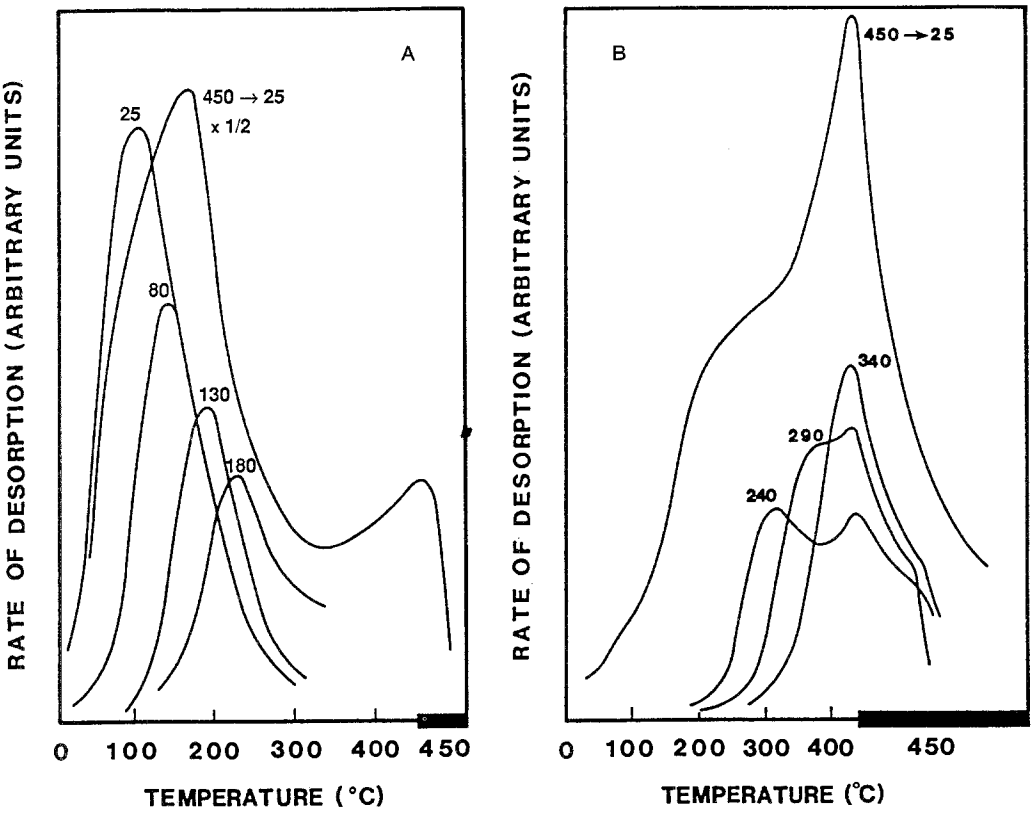

Fig. 7. (A). TPD spectra of hydrogen from 15% Fe/silica (dried 60–80 °C prior to reduction) as a function of adsorption temperature. Solid bar indicates temperature hold at 450 °C. (B). TPD spectra of hydrogen from 15% Fe/silica (dried 100 °C prior to reduction) as a function of adsorption temperature ([ref. [24]). (C). TPD spectra of hydrogen from 15% Fe/3% K/silica as a function of adsorption of temperature. Solid bar indicates temperature hold at 450 °C ([ref. [24]).

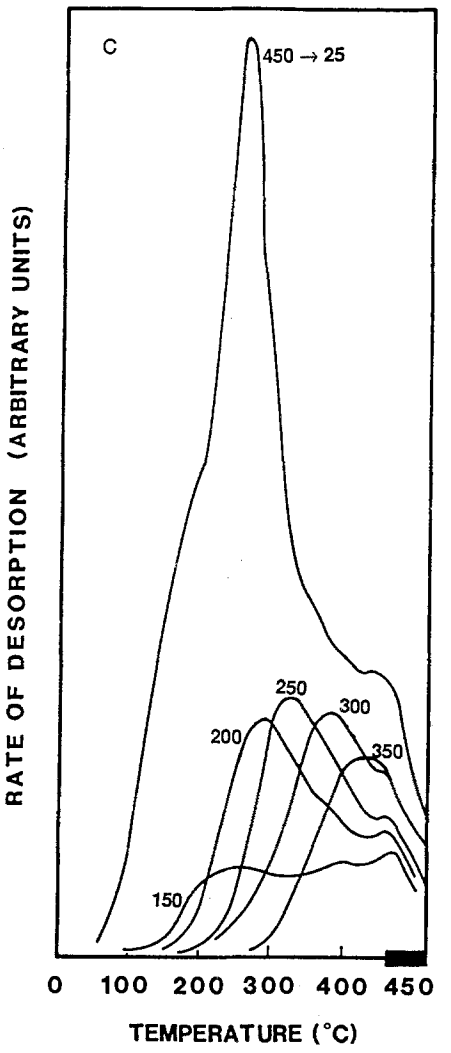

Fig. 7. C.

cobalt [39] are suspect because a good portion of the activated state was excluded from study due to kinetic limitations.

While the activation energies for desorption do not vary greatly with support, significant differences are observed in the heats of adsorption (table 2). Indeed, the heat of adsorption for 10% Co/alumina of 105 kJ/mole is clearly very significantly lower than for either 10% Co/silica or unsupported cobalt (145 kJ/mole for both). The significantly different adsorption enthalpy for Co/alumina is due to its much higher activation energy, which can probably be ascribed as in the case of nickel to the presence of cobalt or aluminum oxide species located either on the cobalt crystallite surface or in intimate contact with cobalt crystallites.

In addition to being influenced by metal-support interactions, the kinetics and energetics of hydrogen adsorption on base metals are influenced by promoters such as potassium [24,31,40], other additives such as carbon, copper and sulfur [27,31,40], and by catalyst preparation/pretreatment methods [24]. Effects of calcination pretreatment and potassium promoter on the adsorption of hydrogen on Fe/silica according to Weatherbee et al. [24] are illustrated in fig. 7.

It is evident from fig. 7a that hydrogen adsorption on a 15% Fe/silica catalyst precalcined at the lower temperature (60–80 °C) prior to reduction for 36 hours in hydrogen is only moderately activated, i.e. a significant quantity adsorbs at 25 °C and the amount adsorbed *decreases* with increasing adsorption temperature; nevertheless the amount adsorbed upon cooling from 450 °C to 25 °C in hydrogen is greater by more than a factor of two than that adsorbed by the pulse method at 25 °C. However, hydrogen adsorption on the catalyst precalcined at the higher temperature (100 °C) is considerably more activated, i.e. negligible hydrogen adsorbs during exposure to pulses of hydrogen at 25–100 °C (fig. 7b). Moreover the amount adsorbed at 150 °C is small and adsorption capacity *increases* with increasing adsorption temperature. It is also evident that the desorption peaks are shifted to higher binding energy with increasing precalcination temperature. Bartholomew et al. [24,36] have attributed these observed increases in adsorption activation and binding energies with increasing precalcination temperature to either (i) contamination during preparation of the iron surface by support species of (ii) the presence of iron oxide either on or in contact with iron metal crystallites. That iron supported on oxide carriers such as alumina, magnesia, and silica cannot be completely reduced to the metallic state and that oxides of iron interact strongly with these supports to form highly stable solid solutions is well documented [24,36,41–45].

TPD spectra for 15% Fe/3% K/silica in fig. 7c when compared with those for 15% Fe/silica in fig. 7a provide evidence that potassium addition likewise increases adsorption activation and binding energies of hydrogen and iron. In addition, a new adsorption state with a maximum at about 400 °C is observed (see fig. 7c). These significant changes in the kinetics and energetics of hydrogen adsorption are explained by localized electronic perturbations of the metal surface by the potassium additives [31,40].

Since promoters and pretreatment methods can separately greatly influence the kinetics and energetics of hydrogen adsorption, it should be interesting to consider effects of simultaneous promotion and pretreatment. The hydrogen TPD spectrum for a 15% Fe/3% K/silica catalyst precalcined before reduction at 200 °C was found to contain no adsorption states below 400 °C [24,36]; in other words, the combined effect of potassium promotion and precalcination is to dramatically increase adsorption activation and binding energies. This substantial change in the hydrogen adsorption properties of this catalyst dramatically affects its activity and selectivity properties in CO hydrogenation [36].

3. Reversibilities and stoichiometries of adsorption

A. REVERSIBLE AND IRREVERSIBLE ADSORPTION

From the TPD data presented in the previous two sections, its is evident that hydrogen adsorption on cobalt, iron and nickel is reversible over a wide range of conditions, i.e. chemisorbed, atomic hydrogen can be desorbed at least in part by evacuation or purging at temperatures above about 200 K. For example, fig. 1, and tables 1 and 2 reveal the existence of atomic hydrogen states of low binding energy on nickel and cobalt which are easily desorbed at temperatures near ambient (200–300 K). The high reversibility of hydrogen adsorption has important implications in regard to proposed techniques for measuring monolayer hydrogen capacities (discussed in section 3C).

It should be emphasized that the term "reversible" or "irreversible" applied to adsorption has operational meaning only. That is, adsorption of hydrogen on nickel at 120–150 K is for all practical purposes "irreversible" since rates of desorption are negligible (see figs. 1 and 3); however at 300 K, the β_1 state of hydrogen on nickel is "reversible" since it is easily desorbed, while the β_2 state is irreversible, that is, not desorbable at measurable rates at this temperature.

Besides TPD studies there have been several previous investigations that provide information on the reversibility of hydrogen adsorption on supported cobalt, iron and nickel catalysts [36,46–49]. These studies, summarized in table 3, provide evidence that the reversibility of hydrogen adsorption is a function of dispersion, support, extent of reduction to the metal, and metal loading. This is reasonable in view of the TPD data presented in the earlier two sections showing that the number of binding states, temperatures for desorption maxima, and binding energies are functions of these same catalyst variables.

The results summarized in table 3 indicate that the percent reversibility of hydrogen adsorbed at 300 K ranges from 10–90% and that the extent of reversibility generally increases with increasing temperature of adsorption, crystallite size, metal loading and with decreasing extent of reduction. The percent reversibility apparently also increases with increasing interaction of support and metal, i.e. in the order M/silica, M/alumina, M/titania, M/carbon, M/magnesia, and with potassium promotion. Hydrogen adsorption is more reversible on catalysts prepared by controlled pH-precipitation relative to those prepared by impregnation. Most of these trends are consistent with and can be explained by the observed shifts in hydrogen desorption states as a result of changes in these catalyst properties which can lead to higher or lower rates of desorption at ambient temperature.

However, other explanations for the observed changes in adsorption reversibility have been proposed which should be mentioned. But the discussion of these other possibilities should be prefaced by a brief review of the facts surrounding

Table 3
Studies of reversible hydrogen adsorption on supported cobalt, iron and nickel catalysts

Ref.	Catalysts	Effects investigated	Observations and comments
[46]	4–40% Ni/ silica	Effects of nickel content and crystallite size on irreversible uptake	Reversibility increases with increasing crystallite size and nickel content.
[47]	3.9% Ni/ alumina 14% Ni/ alumina	Pressure dependence of isotherm Fraction of monolayer desorbing at 300 K	Isotherm pressure dependence increases with decreasing loading. 40% of ML desorbs at 300 K.
[48]	20–30% Ni/ silica 7% Ni/ alumina	Effects of temperature, pressure, support unreduced nickel, and crystallite size	Reversible fraction increases with increasing time and pressure. Reversibility increases with increasing temperature, decreasing extent of reduction, increasing crystallite size, and with change of support form silica to alumina.
[49]	1–15% Co/ alumina 3 & 10% Co on silica, titania, C, and MgO	Effects of support, cobalt content, preparation, and extent of reduction at 300 K	Percent reversibility ranges from 15–90%. Reversibility increases with decreasing extent of reduction and in the order Co/silica, Co/alumina, Co/titania, Co/C, Co/MgO. Reversibility is greater for catalysts prepared by ppt. relative to impregnation and for catalysts of lower loading.
[36]	15% Fe/silica 15% Fe/0.2–3% K/silica	Effects of potassium on reversibility at 300 K	Potassium addition increases percentage reversibility from about 13% to 25–30%.

the behavior of hydrogen adsorption on supported metals. Nickel supported on alumina or silica provides a representative example.

Hydrogen adsorbs on supported nickel at room temperature and pressures of 100–400 Torr in three stages [47,48,50,51]: (i) much (50–80%) of the hydrogen is adsorbed rapidly (within 5 minutes), (ii) a significant quantity is adsorbed within the next 30–45 minutes at which point in time near-equilibrium is achieved, and (iii) a small quantity (typically 3–5% of a monolayer) is taken up very slowly over the next few hours.

Previously reported isotherms [48,51] are consistent with a Langmuir model involving dissociative adsorption on strong sites followed by adsorption on weaker sites. Reversible adsorption on weaker sites would account for the observed increasing adsorption capacity with increasing pressure observed for Ni/silica [48]. Indeed, Richardson and Cale [48] were able to fit their isotherms for Ni/silica with a high degree of confidence to an equation of the form:

$$N_A = N_0 + bP_H^{0.5} \quad (1)$$

where N_A is the number of moles adsorbed at a given pressure, N_0 is the moles adsorbed at zero pressure or in other words strongly adsorbed hydrogen and b is

Table 4
Phenomena proposed to explain reversible adsorption on nickel (refs. [47–51])

Phenomenon	Basis for explanation	Confirming or discounting evidence
1. Decreasing heats with increasing coverage.	Lower binding energies at higher coverages lead to reversible adsorption.	This model fits experimental data very well. Supported by TPD and magnetic data.
2. Adsorption on support or nickel oxide.	Although adsorption on supports or NiO is negligible, Ni crystallites may create new adsorption sites. Physical adsorption.	Magnetic data indicate adsorption occurs on the metal, not the support or nickel oxide. Physical adsorption can be corrected for by extrapolation to $P = 0$.
3. Spillover of atomic hydrogen onto support of nickel oxide.	Hydrogen atoms can diffuse from metal to support.	Large body of evidence confirms occurrence of spillover, but process is slow (requires many hours at 300 K).
4. Reaction with adsorbed contaminants such as oxygen.	Reaction of hydrogen with adsorbed oxygen has been observed [56].	This kind of contamination can be can be avoided. Reaction is not reversible [56].
5. Decoration of metal crystallites by reduced species from the support (socalled "SMSI" effect)	Adsorption on reduced support species or support "skin" located on the surface of metal crystallites could create new sites for reversible adsorption.	Evidence for contamination of metal by reduced support species is well documented. Effects can be minimized by careful preparation. Adsorption on these species is very slow [17,18].
6. Surface inaccessibility.	"Support skin" or pore trapping causes weak, reversible adsorption.	Same as 5 above. No concrete evidence for "pore trapping."
7. Multilayer adsorption.	Greater than monolayer adsorption on bridge or hole positions or predissociative molecular adsorption at high coverages.	TPD studies [7–18] indicate this occurs only at $T < 150$ K.
8. Absorption into the bulk metal.	Penetration into bulk metals could be reversible and slow.	Measured permeation rates into Ni are negligible [52].

a constant which reflects the degree of reversibility. The parameter b increases with decreasing nickel content and decreasing extent of reduction and is larger for Ni/alumina than for Ni/silica [48,51].

While adsorption on sites of at least two different binding energies clearly explains the observed pressure dependence and hence the reversibility of hydrogen adsorption, there are a number of other explanations that have been proposed in previous studies [48], most of which are summarized in table 4. Of these, only absorption into the metal can be entirely discounted, since permeation rates

into nickel are negligibly small [52]. Most of the others involve phenomena observed occasionally and/or which contribute only in small measure to reversibility. For example, the effects of spillover leading to adsorption on the support or unreduced nickel can be neglected in procedures involving a short (e.g. 45 minute) equilibration, since spillover to the oxide phases is a slow, multihour process [17,18,53]; accordingly, the very slow hydrogen uptake observed in "Phase Three" after the initial 45 minute equilibration is most probably due to spillover. Problems of surface contamination and/or surface inaccessibility can be avoided or minimized in most supported base-metal systems through careful preparation and pretreatment. The TPD data in section 2 showed that multilayer or "predissociative" adsorption does not occur above about 120–150 K. The amount of hydrogen that adsorbs strongly on supports under typical conditions is negligible [54], while the contribution of physically adsorbed hydrogen can be eliminated through proper extrapolation of the data (see sections 3.2 and 3.3). Thus, all of the proposed contributions to reversible hydrogen adsorption in table 4 can be discounted with the exception of No. 1, involving different adsorption states or strengths. It is the most reasonable and likely explanation because: (i) it is the only one that can, by itself, explain the data, i.e. it provides a very good fit of the isotherm data using eq. (1) and (ii) it is strongly supported by evidence from TPD and magnetics measurements. The TPD evidence, discussed in section 2, is entirely consistent with the view of different adsorption states or sites of different energies. Magnetic studies [48,55] reveal that changes in the magnetic moment of nickel continue to occur with increasing hydrogen pressure, even up to hundreds of atmospheres, indicating that reversible hydrogen adsorption takes place on nickel crystallites rather than on the support, support contaminant, or unreduced nickel.

B. ADSORPTION STOICHIOMETRIES

1. Adsorption stoichiometries of hydrogen on nickel

There is reliable evidence from the previous literature that hydrogen adsorbs on single crystal nickel [11,12] and polycrystalline nickel [55,56] with a stoichiometry of one hydrogen atom per nickel surface atom. For example, Pannell et al. [56] obtained a H/Ni_s *ratio of 1.1* by comparing the surface area of a high purity nickel powder calculated *from the total hydrogen uptake at 300 K* (based on an equally weighted average of the planer site densities for the 3 lowest index planes) with surface areas determined from argon and nitrogen BET measurements (assuming argon and nitrogen areas of 0.169 and 0.162 nm^2/molecule respectively).

Bartholomew and Pannell [47] investigated the stoichiometries of hydrogen and CO adsorptions on alumina- and silica-supported nickel catalysts having a range of metal loadings, dispersions, and extents of reduction. Their data for catalysts reduced at 725 K provide evidence that (i) *room temperature hydrogen adsorption*

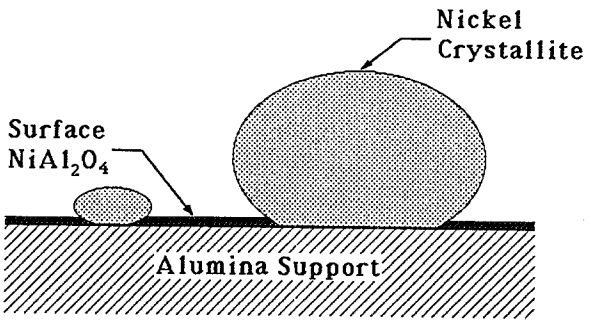

Fig. 8. Model of partially reduced Ni/alumina catalyst ([ref. [47]).

occurs on Ni / alumina and Ni / silica catalysts of moderate or high loading with a stoichiometry of one hydrogen atom per surface nickel atom, if the total adsorption (reversible and irreversible) is included and (ii) less than a monolayer of hydrogen is adsorbed ($H/Ni_s < 1$) on Ni/alumina catalysts of low loading (< 3 wt.%). The first conclusion is supported by the good to very good agreement of particle size estimates from hydrogen adsorption (assuming $H/Ni_s = 1$), X-ray diffraction (XRD) and transmission electron microscopy (TEM) for 14 and 23% Ni/alumina and 13.5 and 15% Ni/silica. Bartholomew and Pannell concluded that the suppression of hydrogen adsorption in catalysts of low loading was due to metal support interactions. Based on the data presented in section 2 it would be reasonable to postulate that strongly activated adsorption and/or contamination of the metal crystallites with support-derived oxides was responsible for this very significant inhibition of hydrogen adsorption.

It should be emphasized that the estimation of metal crystallite size from hydrogen uptake requires that assumptions be made regarding metal crystallite morphology and location of the unreduced metal oxide. Bartholomew and Pannell [47] assumed the metal to be present as spherical nickel crystallites while unreduced nickel oxide was assumed to exist in separate thin layers in intimate contact with the support (see fig. 8). The presence of dense, spherical crystallites of nickel in their catalysts was confirmed by TEM [57]. A stable, hardly-reducible surface nickel aluminate phase in the form of a monolayer on the alumina support is consistent with recently reported ESCA and ISS data [30]. Thus, the model used by Bartholomew and Pannell [47] appears to be consistent with recent morphological information.

Several studies [57–61] provide evidence that significantly less than a monolayer of hydrogen is adsorbed on Ni/titania and that the H/Ni_s ratio decreases with increasing reduction temperature and decreasing nickel loading. The recent evidence is most consistent with blocking of adsorption by reduced support species, TiO_x, that migrate onto crystallites during reduction [17,18]. However, Xuan-Zhen et al. [53] observed a H/Ni_s ratio of one after adsorbing hydrogen on Ni/titania for 15–20 hours; this was attributed to spillover of atomic hydrogen

from the metal to the reduced TiO_x or to the support in contact with the crystallites.

Some previous works [1,48,63] attribute nonstoichiometric adsorption to "limited accessibility" of hydrogen to the metal surface. Access of hydrogen to the surface of a metal crystallite may be affected by (i) the degree to which the metal crystallite contacts or "wets" the support, (ii) the presence on the metal crystallite of contaminants such as carbon, sulfur, or support species, and (iii) collapse of pores accompanied by encapsulation of crystallites during sintering at high temperatures. That reduced support species can migrate onto the surface of Ni/titania during high temperature reduction or be deposited on the nickel crystallites during preparation of Ni/alumina and Ni/silica catalysts is confirmed from several recent investigations [17,18,62]. Recent studies [63–65] also confirm that sintering at high temperatures of Ni/alumina and Ni/silica leads to partial collapse of the micropore structure with encapsulation of nickel crystallites. Nevertheless the data of Bartholomew and Pannell [47] indicate that *hydrogen is essentially completely accessible to the nickel surface in Ni / alumina and Ni / silica catalysts of moderate loading, reduced at 725 K* and which are prepared from high purity supports. While several studies [1,48,63] have reported limited accessibility of hydrogen for unsintered, moderately-loaded nickel catalysts, these results must be questioned, since in most of these studies only strongly adsorbed hydrogen was accounted for; from the previous discussion of reversibility it is clear that this would have led to large (30–90%) errors in the measurement of saturation coverage. For example, Desai and Richardson [63] used a flow technique which measured only the strongly-held hydrogen, while Richardson and Cale [48] used Equation 1 to subtract out the contribution of reversible adsorption. Thus, much of the previous work reporting inaccessibility needs to be revised.

2. Adsorption stoichiometries of hydrogen on cobalt and iron

Hydrogen adsorption measurements on supported cobalt and iron are complicated by high adsorption activation energies which severely limit the rate of adsorption at room temperature. In fact, negligible hydrogen were observed to adsorb on 3–9% Co/ZSM-5 catalysts at 300 K even after a 45 minute equilibration, although 10–100 times as much adsorbed at 100 °C [34].

Reuel and Bartholomew [49] obviated the problem of activated adsorption and *observed monolayer hydrogen adsorption with a stoichiometry of one hydrogen atom per cobalt surface atom on unsupported cobalt. 3 and 10% Co / sillica, and 10 and 15% Co / alumina,catalysts* reduced at 623–673 K *by measuring total hydrogen adsorption at 373–423 K.* The basis of their observation was good to very good agreement of average crystallite diameters estimated from hydrogen adsorption (assuming $H/Co_s = 1$), XRD, and TEM. However, in the case of Co/titania, the

crystallite diameter estimated from hydrogen adsorption was a factor of two higher than that estimated by the other techniques; this poor agreement is attributed to decoration of the metal crystallites by reduced TiO_x species as observed in the Ni/titania system [17,18].

In their investigation of hydrogen adsorption on a 15% Fe/silica catalyst reduced at 725 K, Rankin and Bartholomew [36] found good agreement among crystallite sizes estimated from hydrogen adsorption (assuming $H/Fe_s = 1$), XRD and TEM, if the total hydrogen adsorption capacity was measured by cooling the sample in a predetermined quantity of hydrogen from 673 K to 300 K followed by isotherm measurements at 300 K. Jones et al. [66] also observed similar good agreement among crystallite diameters of 10% Fe/carbon measured by the same three techniques and using a similar procedure for measuring hydrogen adsorption capacity. Thus, it is safe to conclude that hydrogen adsorbs with a $H/M_s = 1$ stoichiometry on conventional cobalt and iron catalysts of moderate or high loading, if the total uptake is measured at elevated temperatures according to the procedures discussed above.

C. MEASUREMENT OF MONOLAYER ADSORPTION CAPACITY

The measurement of monolayer hydrogen adsorption capacity of supported metals is useful in providing estimates of metal surfaces area, average crystallite diameter, and the number of potential catalytic sites available for reaction. The *ideal method* for measuring monolayer adsorption capacity would involve *reproducible, convenient, and rapid* measurements using an apparatus that is easily and economically fabricated; *it must account for hydrogen that is either reversibly or irreversibly chemisorbed on the metal while excluding chemical and physical adsorptions on the support*. Finally it *should provide a means of circumventing the kinetic limitations of highly activated adsorption*. Of course, the measurement of an adsorbed monolayer can only be realized *in the absence of surface contaminants*, e.g. carbon, sulfur and/or reduced support moieties.

Based on the discussions in the two previous sections it is clear that *hydrogen adsorbs in a well-defined monolayer on supported cobalt, iron and nickel* with a stoichiometry of one hydrogen atom per metal surface atom, *if the measurement includes the total (reversible and irreversible) quantity chemisorbed*. Reproducible, convenient static, volumetric methods that have been developed and demonstrated for measuring monolayer hydrogen adsorption capacity on supported nickel, cobalt, and iron catalysts are summarized in table 5. These methods are modifications of the standard procedure for measuring hydrogen chemisorption on Pt developed by Committee D-32 of ASTM [67]; the most significant differences are the procedures developed to circumvent the limitations of highly activated adsorption by means of a high temperature adsorption in the case of cobalt and the cooling in hydrogen from just below the reduction temperature in the case of iron, the latter procedure having been first suggested by Amelse et al.

Table 5
Demonstrated volumetric, static methods for measuring monolayer hydrogen adsorption capacities of supported nickel, cobalt and iron catalysts

Catalysts	Pretreatment	Equilibration and Isotherm Conditions	Limitations
Ni/ alumina	Reduce 15 h at 673–723 K.	Equilibrate 45 min. at 300 K, 350 Torr. Desorption isotherm [b] from 350 to	Metal loadings must be > than 3 wt.%.
Ni/ silica	Evacuate 1 h at −20 K of redn. T [a].	100 Torr. Extrapolate isotherm to $P = 0$ [c].	If adsorption is slow, equil. at 323 K. Measure *total* uptake [d].
Co/ alumina	Reduce 15 h at 673–723 K.	Equilibrate 45 min at 400 K, 350 Torr. Desorption isotherm [b] from 350 to	Metal loadings of > 3% for Co/silica and > 10% for Co/alumina.
Co/ silica	Evacuate 1 h at −20 K of redn. T [a].	100 Torr. Extrapolate isotherm to $P = 0$ [c].	Measure *total* uptake [d].
Fe/ silica	Reduce 36 h at 723 K. Evacuate 1 h at −20 K of redn. T [a].	Cool in measured amt of hydrogen (350 Torr) from −20 K of redn T to 300 K. Desorption isotherm [b] at 300 K from 350 to 100 Torr. Extrapolate isotherm to $P = 0$ [c].	Metal loadings > 15%. Measure *total* uptake [d].

[a] Short evacuation at slightly lower than reduction temperature avoids contamination of metal with water from support, pump oil, etc.
[b] Desorption isotherm is more linear than adsorption isotherm and can be obtained with 30–60 min (5–10 min/point) compared to 4–6 h (45–60 min/point) for adsorption isotherm.
[c] Extrapolation eliminates contribution of physical adsorption or erroneous dead volume.
[d] Total uptake is the extrapolated uptake which includes reversible and irreversible adsorption.

[68]. The procedure for nickel was tested on a commercial 12% Ni/alumina catalyst by a task force of the ASTM Committee D-32 in a round-robin involving 8 laboratories with a standard deviation of only ±7% [69], which is well within the limits of error for conventional volumetric adsorption procedures.

Some of the assumptions underlying the choice of conditions or procedures as well as the limitations of the methods are also briefly summarized in table 5. Some further clarification is appropriate here. Because of the strong interaction of base metal oxides with alumina [29,30] and of iron with silica [36], a 15 hour reduction at 673–725 K is recommended for nickel and cobalt catalysts and a 36 hour reduction for Fe/silica. These recommendations are based on measurements of the extent of reduction as a function of reduction time [29,36,47,49]. The relative short evacuation time of 1 hour is chosen to avoid contamination of the metal surface by pump oil, water or other such contaminants that might be present in the vacuum manifolds or traps and is based on experience from many laboratories too numerous to mention. The purpose of evacuating at a slightly lower temperature than that used in the reduction is to avoid oxidation of the metal surface by water from the support, since it is well known that water can be removed incrementally by dehydroxylation of alumina and silica supports up to

temperatures as high as 1200 K [70]. In fact, it was recently reported [71] that a lengthy evacuation of Pt/silica at a temperature higher than that of the reduction resulted in oxidation of a portion of the platinum, while there was no observable change in the state of reduction as measured by Mössbauer spectroscopy of a well-dispersed 1% Fe/carbon reduced at 673 K upon evacuation for 1 hour at 653 K [72]. The equilibration at a relatively high pressure of 350 Torr ensures that equilibrium will be attained within about 45 minutes [36,47,49,51]. By measuring the isotherm in increments of decreasing pressure (desorption method) it is generally possible to measure isotherm points every 5–10 minutes, while the adsorption method (increments of increasing pressure) may require waiting 45 minutes or longer for each point to reach equilibrium; moreover, the isotherm obtained by the desorption method is generally more linear than that obtained by the adsorption method [73]. Besides the enormous savings in time the desorption method avoids complications due to spillover that generally occur over a period of hours [17,18,53]. Because physical adsorption of hydrogen can occur on typical supports even at 300–400 K and because errors in the determination of the dead volume (cell and manifold volume) can cause significant variations in the isotherm slope, it is necessary to extrapolate the linear portions of the isotherm to zero pressure.

The methods described in table 5 are generally limited to alumina- and silica-supported cobalt, iron and nickel catalysts of moderate or high loading ($>$ 3% for Ni/silica and Co/silica and $>$ 10% for Ni/alumina, Co/alumina, and Fe/silica) since at lower loadings metal contamination by reduced support moieties, spreading of the crystallite on the support, or other forms of metal-support interactions limit accessibility of hydrogen to the metal surface. Thus, these methods cannot be applied with any confidence to catalysts of low metal content nor to catalysts involving highly reducible supports such as titania or contaminating supports such as carbon without first establishing experimentally the conditions (if any) under which monolayer adsorption occurs.

While the methods described in table 5 can be performed conveniently with conventional vacuum adsorption apparatus within 2–3 hours following the completion of the pretreatment, reduction and evacuation, there is clearly interest in developing faster, more convenient flow techniques for measuring hydrogen adsorption on supported metals. Unfortunately, previously proposed pulse-flow [63,74] or flow-desorption [68] techniques involve a purge at 273–300 K that removes reversibly chemisorbed hydrogen; thus, the resultant estimate of hydrogen adsorption capacity is low by 30–50%, since typically 30–50% of the adsorbed hydrogen is easily desorbed under these conditions (see sections 2 and 3.1). A new method [75] involves cooling the reduced catalyst in hydrogen to about 200 K, purging with argon at 200 K, and continuing the purge in argon while the temperature is raised to 673 K; the amount of hydrogen originally adsorbed on the catalyst is determined from the area under the desorption peak. In principle, this technique should provide an accurate measure of monolayer

capacity, since the initial purge is conducted below the temperature at which atomic states of hydrogen typically desorb.

4. Summary

In this paper, some of the fundamentals of the kinetics, energetics, reversibilities, and stoichiometries of hydrogen adsorption on supported cobalt, iron and nickel catalysts were presented and discussed in the light of presently available data. Several important issues relating to (i) the relationship of catalyst and adsorption properties and (ii) the application of hydrogen chemisorption to the measurement of metal surface areas were discussed. The present evidence supports the following conclusions:

1. The kinetics and energetics of hydrogen adsorption on cobalt, iron and nickel are apparently little affected by metal surface structure but are significantly changed by metal-support interactions, particularly in catalysts of low metal content or involving highly reducible supports such as titania. Contamination of the metal surface by support moieties, spreading of the metal on to the support or other forms of metal-support interactions because (i) the appearance of new adsorption states of hydrogen at higher binding energies and (ii) an increase in the adsorption activation energy for hydrogen which can lead to severe kinetic limitations in the adsorption process.

2. Precalcination treatments and promoters such as potassium also cause the appearance of new high temperature adsorption states and significantly increase the adsorption activation energy for hydrogen. The appearance of new strongly bound states of hydrogen due to pretreatment, support, and promoter effects may cause unusual changed in catalyst activity and selectivity [1,36].

3. Hydrogen adsorption on cobalt, iron and nickel is generally highly reversible at room temperature because of the existence of an atomic adsorption state which is easily desorbed at 200–300 K. The reversibility of hydrogen adsorption on supported metals varies from 15–90% and increases with increasing temperature, crystallite size, metal content and with decreasing extent of reduction. Hydrogen adsorption is more reversible on alumina-supported metals relative to silica-supported metals.

4. Hydrogen chemisorbs on Ni/alumina and Ni/silica catalyst of moderate loadings at 300 K and 100–350 Torr with a stoichiometry of one hydrogen atom per nickel surface atom, if the adsorption method accounts for the total of reversible and irreversible chemisorption. A well-defined monolayer ($H/M_s = 1$) is also observed on cobalt and iron catalysts of similar loadings and supports, if the total uptake is measured at 400 K or by cooling in hydrogen from about 673 K to 300 K in order to circumvent the limitations of highly activated adsorption. Under these conditions there is no evidence for "limited accessibility" of hydrogen to the metal surface for these nickel, cobalt, or iron catalysts.

5. Less than monolayer adsorption is observed on cobalt, iron and nickel catalysts of low metal content or supported on high reducible supports such as titania. These results are consistent with contamination of the metal by support species during preparation or reduction.

6. Static, volumetric methods for measuring monolayer hydrogen adsorption capacity have been demonstrated for alumina- and silica-supported cobalt, iron, and nickel catalysts of moderate loadings. With two exceptions [68,75] previously proposed pulse-flow or flow techniques measure only irreversibly chemisorbed hydrogen and are therefore *not* recommended.

References

[1] *Hydrogen Effects in Catalysis*, eds. Z. Paal and P.G. Menon (Marcel Dekker, Inc., N.Y., 1988).
[2] I. Toyoshima and G.A. Somorjai, Catal. Rev.-Sci. Eng. 19 (1979) 105.
[3] O. Beeck, Adv. Catal. 2 (1951) 151.
[4] M. Wahba and C. Kemball, Trans. Farad. Soc. 49 (1953) 1351.
[5] D.F. Klemperer and F.S. Stone, Proc. R. Soc. London A243 (1957) 375.
[6] D. Brennan and F.H. Hayes, Trans. Farad. Soc. 60 (1964) 589.
[7] F.J. Broecker and G. Wedler, Disc. Farad. Soc. 47 (1966) 87.
[8] J. Lapujoulade and K.S. Neil, Surf. Sci. 35 (1972) 288; J. Chem. Phys. 70 (1973) 798.
[9] J. McCarty, J. Falconer and R.J. Madix, J. Catal. 30 (1973) 235.
[10] K. Christmann, O. Schober, G. Ertl and M. Neumann, J. Chem. Phys. 60 (1974) 4528.
[11] K. Christmann, Z. Naturforsch. A, 34 (1979) 22.
[12] A. Winkler and K.D. Rendulic, Surf. Sci. 118 (1982) 19.
[13] N.M. Popora, L.V. Babenkova and Sokol'skii, Kinet. Katal. 10 (1969) 1171.
[14] J.A. Konvalinka, P.H. Van Oeffelt and J.J.F. Scholten, Appl. Catal. 1 (1981) 141.
[15] P.I. Lee and J.A. Schwarz, J. Catal. 73 (1982) 272.
[16] G.D. Weatherbee and C.H. Bartholomew, J. Catal. 87 (1984) 55.
[17] G.B. Raupp and J.A. Dumesic, J. Catal. 95 (1985) 587.
[18] G.B. Raupp and J.A. Dumesic, J. Catal. 97 (1986) 85.
[19] E.E. Ibok and D.F. Ollis, J. Catal. 66 (1980) 391.
[20] R.K. Herz, J.B. Kiela and S.P. Marin, J. Catal. 73 (1982) 66.
[21] R.J. Gorte, J. Catal. 75 (1982) 164.
[22] J.L. Falconer and J.A. Schwarz, Catal. Rev.-Scie. Eng. 25 (1983) 141.
[23] J.S. Rieck and A.T. Bell, J. Catal. 85 (1984) 143.
[24] G.D. Weatherbee, J.L. Rankin and C.H. Bartholomew, Appl. Catal. 11 (1984) 73.
[25] A. Clark, *The Theory of Adsorption and Catalysis*, (Academic Press, New York, 1970) p. 211.
[26] J.K. Roberts, Proc. Roy. Soc. (London). Ser. A. 152 (1935) 445.
[27] K.B. Kester and J.L. Falconer, J. Catal. 89 (1984) 380.
[28] J.-G. Choi, H.-K. Rhee and S.H. Moon, Appl. Catal. 13 (1985) 269.
[29] C.H. Bartholomew and R.J. Farrauto, J. Catal. 45 (1976) 41.
[30] M. Wu and D.M. Hercules, J. Phys. Chem. 83 (1979) 2003.
[31] R.J. Madix, Catal. Rev. -Sci. Eng. 15 (1977) 293.
[32] J. Dollimore and B. Harrison, J. Catal. 28 (1973) 275.
[33] J.M. Zowtiak and C.H. Bartholomew, J. Catal. 82 (1983) 230.
[34] J.M. Zowtiak and C.H. Bartholomew, J. Catal. 83 (1983) 107.
[35] Y. Amenomiya and G. Pleizier, J. Catal. 28 (1973) 442.

[36] J.L. Rankin and C.H. Bartholomew, J. Catal. 100 (1986) 526, 523.
[37] R. Rudham and F.S. Stone, Trans. Farad. Soc. 54 (1958) 421.
[38] R. Dus and W. Lisowski, Surf. Sci. 61 (1976) 635.
[39] M.E. Bridge, C.M. Comrie and R.M. Lambert, J. Catal. 58 (1979) 28.
[40] J. Benzinger and R.J. Madix, Surf. Sci. 94 (1980) 119.
[41] M.C. Hobson and A.D. Campbell, J. Catal. 8 (1967) 294.
[42] R.L. Garten and D.F. Ollis, J. Catal. 35 (1974) 232.
[43] M. Boudart, A. Delbouille, J.A. Dumesic, S. Khammouma and H. Topsoe, J. Catal. 37 (1975) 486.
[44] I. Sushumna and E. Ruckenstein, J. Catal. 94 (1985) 239.
[45] A.J.H.M. Kock, H.M. Fortuin and J.W. Geus, J. Catal. 96 (1985) 261.
[46] A.A. Slinkin, A.V. Kucherov and A.M. Rubenshtein, Kinetics and Catalysis 19 (1978) 415.
[47] C.H. Bartholomew and R.B. Pannell, J. Catal. 65 (1980) 390.
[48] J.T. Richardson and T.S. Cale, J. Catal. 102 (1986) 419.
[49] R.C. Reuel and C.H. Bartholomew, J. Catal. 85 (1984) 63.
[50] J.R. Rostrup-Nielsen, J. Catal. 11 (1968) 220.
[51] C.H. Bartholomew, "Alloy Catalysts with Monolith Supports for Methanation of Coal-Derived Gases," Final Technical Report to ERDA, FE-1790-9, Sept. 6, 1977.
[52] R.B. McLellan and C.G. Harkins, Mater. Sci. 18 (1975) 5.
[53] J. Xuan-Zhen, T.F. Hayden and J.A. Dumesic, J. Catal. 83 (1983) 168.
[54] R.C. Reuel, M.S. Thesis, Brigham Young University, 1983.
[55] P.W. Selwood, J. Catal. 42 (1976) 148.
[56] R.B. Pannell, K.S. Chung and C.H. Bartholomew, J. Catal. 46 (1977) 340.
[57] D.G. Mustard and C.H. Bartholomew, J. Catal. 67 (1981) 186.
[58] C.H. Bartholomew, R.B. Pannell and J.L Butler, J. Catal. 65 (1980) 335.
[59] M.A. Vannice and R.L. Garten, J. Catal. 56 (1979) 236.
[60] J.S. Smith, P.A. Thrower and M.A. Vannice, J. Catal. 68 (1981) 270.
[61] E.I. Ko, S. Winston and C. Woo, J. Chem. Soc. Chem. Commun. (1982) 741.
[62] P. Turlier, J.A. Dalmon and G.A. Martin, in: *Metal-Support and Metal-Additive Effects in Catalysis*, eds. B. Imelik et al. (Elsevier Scientific Publishing Co., 1982) pp. 203–210.
[63] P. Desai and J.T. Richardson, in: *Catalyst Deactivation*, eds. B. Delmon and G.F. Froment (Elsevier Scientific Publishing Co., 1980) pp. 149–158.
[64] C.H. Bartholomew, R.B. Pannell and R.W. Fowler, J. Catal. 79 (1983) 34–46.
[65] C.H. Bartholomew and W.L. Sorensen, J. Catal. 81 (1983) 131.
[66] V.K. Jones, L.R. Neubauer and C.H. Barthomolew, submitted for publication, 1986.
[67] ASTM Committee D-32, "Standard Test Method for Hydrogen Chemisorption on Supported Platinum on Alumina Catalysts by Volumetric Vacuum Method," D-3908-82, in: *1985 Annual Book of ASTM Standards* 5 (1985) 940.
[68] J.A. Amelse, L.H. Schwartz and J.B. Butt, J. Catal. 72 (1981) 95.
[69] C.H. Bartholomew, "Progress Summary of Results for the First Round-Robin Testing of the Proposed ASTM Procedure for Measurement of Nickel Surface Area," prepared for: Metal Dispersion Task Force, November 9, 1976.
[70] J.B. Peri, J. Phys. Chem. 69 (1965) 211.
[71] A. Frennet and P.B. Wells, Appl. Catal. 18 (1985) 243.
[72] L.R. Neubauer and C.H. Bartholomew, paper in preparation.
[73] C.H. Bartholomew, Unpublished data.
[74] E.A. Verma and D.M. Ruthven, J. Catal. 19 (1970) 401.
[75] R.D. Jones and C.H. Bartholomew, Appl. Catal. 39 (1988) 77–88.